8 Week Report

Hersh Aditya Samdani ep22b027

July 2024

Acknowledgements

I would like to express my sincerest gratitude to the Indian Academy of Sciences for this invaluable opportunity to participate in such a concerted interdisciplinary research project where I was able to learn not only physics but also essentials of material science such as DFT. I am deeply to Prof. Nirat Ray for her insight and constant help throughout the endeavour.

I would also like to thank the PhD scholars in the lab, especially Dr. Kiran whose PhD defence I had the privilege to watch and Mr. Manjeet Godara.

I would also like to thank my family and friends who have always supported me unconditionally and who gave me company throughout the summer.

1 Introduction

Condensed matter physics is the branch of physics that deals with the properties and phases of matter on both a microscopic and macroscopic level. An exciting and upcoming research field is that of *Topological States of Matter*. The field started off with the discovery of the *Quantum Hall Effect* by von Klitzing [1] in 1980, followed by the *fractional Quantum Hall Effect* discovered by Tsui et al [2] in 1982. The third paradigm-shifting discovery that is essential for topological states was that of *High Temperature Superconductivity* by Bednorz [3] in 1986. The last two discoveries are out of the scope of this report but it is enough to say that the inability of symmetry breaking to explained them is what led to the establishment of the field of topological states of matter.

Through the course of this two month internship, I studied quantum transport through various physical systems, specifically using a python library called *Kwant*.

2 Quantum Transport

2.1 Scattering Matrix

The scattering matrix is a crucial concept that connects the incoming and outgoing states in a conductor. This matrix is a fundamental element computed in mesoscopic transport simulations and encapsulates the key properties of such systems.

Consider a coherent conductor with N attached leads or terminals. The total number of modes at a given energy E can be expressed as the sum of the modes in each individual lead:

$$M(E) = \sum_{j=1}^{N} M_j(E),$$

where $M_j(E)$ represents the number of modes at energy E in lead j.

The scattering matrix S is an $M \times M$ matrix that connects the amplitudes of the incoming and outgoing modes in the leads. Let $\mathbf{a}$ and $\mathbf{b}$ be $M \times 1$ matrices containing the amplitudes of incoming and outgoing modes, respectively. The relationship is given by:

$$\mathbf{b} = S\mathbf{a}.$$

For current conservation, the total incoming probability must equal the total outgoing probability, i.e., $\sum_m |a_m|^2 = \sum_m |b_m|^2$. This can be expressed as $\mathbf{a}^\dagger\mathbf{a} = \mathbf{b}^\dagger\mathbf{b}$. From this, it follows that the scattering matrix S must be unitary.

A key application of the scattering matrix is in determining the transmission probability of an electron from lead k to lead j (denoted as T_{jk} in Eq. 1.24). This transmission probability can be written in terms of S as:

$$T_{jk}(E) = \sum_{n,n'} |S_{nn'}|^2.$$

The unitarity of S implies that $\sum_{m=1}^{M} |S_{mn}|^2 = 1$, ensuring that an electron entering through mode n will always exit the conductor, thus preserving the total probability.

2.2 Tight - Binding Models

This section aims to discuss the methods used in quantum transport simulations of *tight binding models*. We use this approximation throughout to study the properties of various systems.

The tight-binding approximation evaluates a Hamiltonian on a discrete lattice. This works well in cases where, for example, a system where each lattice point corresponds to an atom. There are also some limitations of the tight binding model which will be elaborated later.

As an example, consider a situation described by the Hamiltonian $\hat{H} = \hat{p}^2/2m$ where $\hat{p} = -\iota\hbar\partial_x = \hbar k$. Let us use a one-dimensional chain of length L with a lattice constant a. The lattice positions are $x = ja$, with $j = 1, 2, ..., N$ and the wave functions can be written as $\psi_j \equiv \psi(x = ja)$. To discretise the derivative while we maintain the hermicity of the Hamilltonian, we ues the symmetric finite difference equation [4]:

$$\hat{p}\,\psi(x)\,|_{x=x_j} = -\frac{i\hbar}{2a}(\psi_{j+1} - \psi_{j-1})$$

and

$$\hat{p}^2\,\psi(x)\,|_{x=x_j} = -\frac{\hbar^2}{a^2}(\psi_{j+1} - 2\psi_j + \psi_{j-1})$$

so the Schrodinger's equation can be rewritten as:

$$t(\psi_{j+1} - 2\psi_j + \psi_{j-1}) = E\psi_j$$

where $t = \hbar^2/2m$ is the *hopping amplitude* and E is the energy. The rewritten form of the Schrodinger equation can be expressed in matrix form and that is the matrix that Kwant takes as an input.

Consider a scattering region with N semi-infinite leads attached to it, labeled by $\alpha = 1, 2, ..., N$ each hosting M_α modes. If we take the scattering region to be described by a single-particle tight-binding Hamiltonian:

$$\hat{H} = \sum_{i,j} H_{i,j} |i\rangle\langle j|$$

Let us consider that the scattering region is only attached to two leads: L, R with $H_L and H_R$ representing the left and right lead Hamiltonians respectively. Hopping beteween the nearest-neighnours are represented by V_L, V_R. For the sake of simplicity we will consider all the other hopping terms to be zero. Then the total Hamiltonian can be represented by:

$$H = \begin{pmatrix} H_L & V_{LS} & 0 \\ V_{SL} & H_S & V_{SR} \\ 0 & V_{RS} & H_R \end{pmatrix}$$

In order to obtain the energies and wave functions, we solve for the eigenvalue of $H\psi = E\psi$, where ψ is the wave function and E is the energy.

$$\begin{pmatrix} H_S - E & V_{TS} & 0 & 0 & \cdots \\ V_{TS}^\dagger & H_T - E & V_T^\dagger & 0 & \cdots \\ 0 & V_T & H_T - E & V_T^\dagger & \cdots \\ 0 & 0 & V_T & H_T - E & \cdots \\ \vdots & \vdots & \vdots & \vdots & \ddots \end{pmatrix} \begin{pmatrix} \psi_S \\ \psi_0 \\ \psi_1 \\ \psi_2 \\ \vdots \end{pmatrix} = \begin{pmatrix} 0 \\ 0 \\ 0 \\ 0 \\ \vdots \end{pmatrix}$$

, Here ψ_S is the wave function of the scattering region and and ψ_i represents the wave function in the *i-th* unit cell in the lead, starting from the scattering region.

2.3 Wave Function Matching

Kwant, uses the *Wave Function Matching (WFM)* approach as the default method to obtain the scattering matrix in transport simulations. The approach solves the scattering problem by matching the fave function at the scattering region with the modes in the leads as the name suggests. In order to solve the above matrix, we introduce an eigenmode basis ϕ_j, with the sub-script signalling the j-th unit cell away from the scattering region. This basis is of dimension M_T, where M_T is the total number of modes in the lead. Therefore we can say:

$$V_T \phi_{j-1} + (H_T - E)\phi_j + V_T^\dagger \phi_{j+1} = 0$$

. The lead is semi-infinite and shows translational symmetry with a period given by a unit cell. If we use Bloch's theorem, we can express our eigenmode as

$$\phi_j = \lambda^j \chi$$

, where $\lambda = e^{ika}$, with k being the wave vector, a the lattice constant and χ is a function that is independent of the unit cell altogether. By out choice of λ we are considering only propagating modes.

Introducing the auxiliary function: $\chi^{'} = \lambda^{-1} V_T \chi$, we get

$$\begin{pmatrix} H_T - E & I \\ V_T & 0 \end{pmatrix} \begin{pmatrix} \chi \\ \chi^{'} \end{pmatrix} = \lambda \begin{pmatrix} -V_T^{\dagger} & 0 \\ 0 & I \end{pmatrix} \begin{pmatrix} \chi \\ \chi^{'} \end{pmatrix}$$

Here, I is the identity matrix.

Through detailed calculations, which are derived in [5] but not shown here, it can be demonstrated that the current associated with a mode n is given by:

$$j_n = -\frac{2}{\hbar} \mathrm{Im}(\lambda_n \chi_n^{\dagger} V_T \chi_n),$$

As utilized in Kwant , we will now distinguish between incoming modes, $j_n > 0$, and outgoing modes, $j_n < 0$. Evanescent modes, which do not carry current, are treated equally in Kwant. However, for the purposes of this thesis, we will ignore them as they do not contribute to the transmission.

We denote incoming modes with a '+' superscript and outgoing ones with a '-'. The next step involves using $\chi_n^{\pm}$ as a basis to express the wave function ψ_j in the j-th unit cell from the scattering region:

$$\psi_j = \sum_n^{N_p} (\lambda_n^-)^j A_n^- \chi_n^- + \sum_n^{N_p} (\lambda_n^+)^j A_n^+ \chi_n^+,$$

where N_p is the number of propagating modes, which is less than or equal to M_T since we are neglecting the evanescent modes, and $A_n^{\pm}$ are the amplitudes of the modes.

We define a scattering matrix $\tilde{S}$ to relate these amplitudes: $A_n^+ = \tilde{S} A_n^-$. The final step is to express the wave function in the lead resulting from the incident mode n as a function of $\tilde{S}$:

$$\psi_{j,n} = (\lambda_n^-)^j \chi_n^- + \sum_{m=1}^{N_p} \tilde{S}_{nm} (\lambda_m^+)^j \chi_m^+.$$

With this, we can rewrite the incident mode n as:

$$(H_S - E)\psi_{S,n} + V_T^{\dagger} \psi_{0,n} = 0, V_{TS} \psi_{S,n} + (H_T - E)\psi_{0,n} + V_T^{\dagger} \psi_{1,n} = 0.$$

The subsequent steps involve extensive mathematical operations, which are not

reproduced here but can be found in [**?**]. Eventually, the following expression is derived:

$$\begin{pmatrix} H_S - E & V_T^\dagger \chi^+ \\ V_{TS} & -\chi'^+ \end{pmatrix} \begin{pmatrix} \psi_S \\ \tilde{S} \end{pmatrix} = \begin{pmatrix} -V_T^\dagger \chi^- \\ \chi'^- \end{pmatrix},$$

with $\psi_S = \begin{pmatrix} \psi_{S,1} & \psi_{S,2} & \cdots & \psi_{S,N_p} \end{pmatrix}$.

It is important to note that $\tilde{S}$ is not the normalized scattering matrix of interest, as it is derived from unnormalized ψ_j and hence is not unitary. The full scattering matrix elements S_{nm} are given by [**?**, **?**]:

$$S_{nm} \equiv \sqrt{\frac{j_n}{j_m}} \tilde{S}_{nm}.$$

Through this, we have shown how to compute the wave function in the scattering region, ψ_S, and the scattering matrix S using the Wave Function Matching (WFM) method. From these, other critical quantities, such as conductance and the density of states, can be derived.

3 Topological Insulators

Topology is a discipline of mathematics that deals with properties of objects that remain unchanged under continuous deformations such as bending or stretching. It is possible to transfer the idea of topology from mathematics in to physics by associating the Hamiltonian of a physical system to the topology of a surface. A good example of a topological invariant used in physics commonly is called the *Chern number C*. It is defined as the intergral of the Berry curvature over the Brillouin zone of a crystal. It behaves like a genus and is unchanging under continuous deformations of the system by definition and so is very robust against perturbations and independent of disorders in the experimental set up. It is in fact this *robustness* that makes materials with topological properties rather interesting for applications in computation and electronics.

Topological Insulators are materials with an ordinary bulk gap, much like a traditional insulator, and gapless conducting edge states that are robust to disorder, like mentioned above. In the case of three-dimensional Topoligcal insulators, the surface state is a two-dimensional electron gas with potential applications in computation, metrology etc.

3.1 Topological States of Matter

Phases of matter have traditionally been described based on the symmetries they break, a phenomenon known as spontaneous symmetry breaking. This

includes examples such as the translation symmetry broken in solids with crystalline structures and the gauge symmetry broken in superconductors. Landau theory characterizes matter using an order parameter, which is a physical quantity that assumes a non-zero value in the ordered phase and zero in the disordered phase. This parameter is essential for analyzing phase transitions. For example, in a ferromagnet, the order parameter is the magnetization.

In contrast, topological states of matter, such as the quantum-Hall and quantum-spin-Hall states, are not described by local order parameters but by topological invariants. These invariants are quantities that take on quantized values and remain unchanged under continuous and smooth transformations of the system's parameters.

This concept can be illustrated using the mathematical classification of two-dimensional surfaces based on their genus. Consider a sphere and an ellipsoid: their surfaces are topologically equivalent because their number of holes (zero) remains constant when one is continuously deformed into the other. Similarly, a cup and a doughnut are topologically equivalent since they both have a genus of one, allowing them to be continuously transformed into one another.

In the realm of quantum systems and topological insulators, this idea translates to the notion that two Hamiltonians are topologically equivalent if they can be adiabatically transformed into each other without closing the band gap. If two materials have different topological invariants, they cannot be adiabatically connected. Consequently, when such materials are brought into contact, the band gap must close at the interface. This leads to the appearance of gapless conducting edge states, known as topological surface states (TSS), at the boundary of the system. Topological surface states are the focus of this study, as a topological insulator nanowire in contact with air or vacuum will exhibit these states, given that air and vacuum are topologically trivial while the topological insulator is not.

3.2 Three-Dimensional Topological Insulators

In three-dimensional topological insulators (3D TIs), the surface states are characterized by a Dirac cone dispersion, which arises from the linear relationship between energy and momentum at the surface. These materials exhibit insulating behavior in the bulk but possess robust, gapless surface states that are protected by time-reversal symmetry. The Hamiltonian describing these surface states typically takes the form

$$\hat{H} = \hbar\nu_F(\hat{k}_x\sigma_x + \hat{k}_y\sigma_y)$$

where ν_F represents the Fermi velocity and σ_x and σ_y are Pauli matrices related

to spin. This Dirac-like dispersion leads to spin-momentum locking, where the electron's spin orientation is locked perpendicular to its momentum, resulting in helical Dirac fermions.

The topological nature of 3D TIs is ensured by a Z_2 invariant, a mathematical property that remains unchanged under continuous deformations of the system, provided time-reversal symmetry is maintained. This invariant guarantees the existence of the surface states and protects them from perturbations such as non-magnetic impurities and structural disorder. Consequently, the surface states of 3D TIs exhibit resilience to backscattering, making them ideal for applications in low-dissipation electronic devices.

Furthermore, the unique properties of 3D TIs open up avenues for realizing novel quantum phenomena. For example, when a 3D TI is placed in proximity to a superconductor, it can host Majorana fermions—quasiparticles that are their own antiparticles and are of great interest for topological quantum computing. The interplay between topological insulators and magnetic materials can lead to the quantum anomalous Hall effect, where edge states carry current without an external magnetic field, promising advancements in spintronics.

Additionally, 3D TIs have been investigated for their potential in thermoelectric applications. The presence of robust surface states contributes to enhanced thermoelectric efficiency, as they can provide high electrical conductivity while maintaining low thermal conductivity. This dual capability makes 3D TIs suitable candidates for energy conversion technologies.

4 Kwant

In this section, we will first define Kwant. It is an open source *Python* package that is used for numerical calculations on tight-binding models and quantum transport simulations[]. It does the calculations by using the wave function matching method, as described in a previous section.

We will now go over a Kwant example, to see how it works at a basic level and then use some of its functionality to simplify the simulation code.

4.1 Conductance for a simple system

In this example we compute the transmission probability through a two-dimensional quantum wire. The wire is described by the two-dimensional Schrodinger equation:

$$H = -\frac{\hbar^2}{2m}(\partial_x^2 + \partial_y^2) + V(y)$$

Where V(y) is a hard wall confinement in the y-direction.

To implement the quantum wire with Kwant, the continuous Hamiltonian H has to be discretized to turn it into a tight-binding mode. For the sake of simplicity, we discretize it on sites of the square lattice with lattice constant a. So, a point with the integer lattice constants (x, y) has the real space coordinates (ai, aj). As we had discussed before, the Hamiltonian becomes

$$H = \sum_{i,j}[(V(ai, aj)+4t)|i, j\rangle\langle i, j|-t(|i+1, j\rangle\langle i, j|)+|i, j\rangle\langle i+1, j|+|i, j+1\rangle\langle i, j|+|i, j\rangle\langle i, j+1|]$$

with

$$t = \frac{\hbar^2}{2ma^2}$$

The code and the explanation are as shown:

```
import kwant
syst = kwant.Builder()
```

Trivially, we first import kwant to enable it. We then define the tight binding system by creating an instance of the *Builder* class.

Naturally, the next stop is to specify the type of sites we want to add to the system. We are using a basic square lattice here. Once again, for simplicity, we set the lattice constatn a to unity.

```
a = 1
lat = kwant.lattice.square(a, norbs=1)
```

In specifying norbs = 1, we tell Kwant that there is 1 degree of freedom.

Now we build a rectangular scattering region that is W lattice points wide and L lattice points wide.

```
t = 1.0
W, L = 10, 30
for i in range(L):
for j in range(W):
syst[lat(i, j)] = 4 * t
if j > 0:
syst[lat(i, j), lat(i, j - 1)] = -t
if i > 0:
syst[lat(i, j), lat(i - 1, j)] = -t
```

This implements the on-site Hamiltonian component:

$$\sum_{i,j}(V(ai, aj) + 4t)|i, j\rangle\langle i, j|$$

And the hopping in the x-direction is:

$$\sum_{i,j} -t(|i + 1, j\rangle\langle i, j| + |i, j\rangle\langle i + 1, j|)$$

They y-direction hopping is represented by:

$$\sum_{i,j} -t(|i, j + 1\rangle\langle i, j| + |i, j\rangle\langle i, j + 1|)$$

The hard-wall confinement that $V(y)$ represents is realised by not having hopping and sites beyond a certain region of space.

Next, we define the leads, here we can use Builder but instead here we take advantage of the translational symmetry:

```
sym_left_lead = kwant.TranslationalSymmetry((-a, 0))
left_lead = kwant.Builder(sym_left_lead)
```

The vector $(-a, 0)$ defines the translational symmetry in a direction away from the scattering region and into the lead.

```
for j in range(W):
left_lead[lat(0, j)] = 4 * t
if j > 0:
left_lead[lat(0, j), lat(0, j - 1)] = -t
left_lead[lat(1, j), lat(0, j)] = -t
syst.attach_lead(left_lead)
```

This finished up adding the left lead. We can define the right lead similarly, but once more Kwant has functionality to attach it more easily.

```
syst.attach_lead(left_lead.reversed())
```

```
kwant.plot(syst);
```

This plots the lattice:

In order to do our transport calculations we finalize the system using $syst.finalized()$.

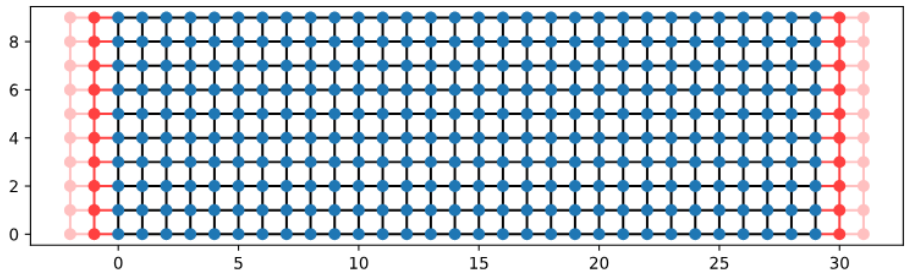


```
energies = []
data = []
for ie in range(100):
energy = ie * 0.01
smatrix = kwant.smatrix(syst, energy)
energies.append(energy)
data.append(smatrix.transmission(1, 0))
```

We can have values of conductance as a function of energy. Plotting the data gives us:

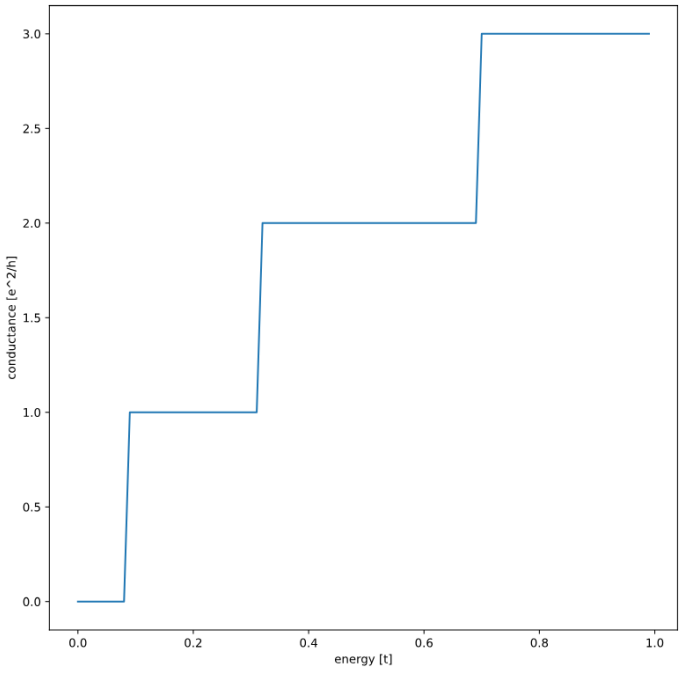

5 Theoretical Framework

The hybrid superconductor-semiconductor nanowire system is a leading candidate for the realization, control, and manipulation of Majorana zero modes (MZMs) for topological quantum information processing. MZMs can be engineered in these hybrid nanowire systems by leveraging the one-dimensional nature of the nanowire, strong spin–orbit coupling, superconductivity, and appropriate external electric and magnetic fields to control the chemical potential and Zeeman energy, respectively, driving the system into a topologically nontrivial phase [6]. To induce superconductivity in the semiconductor nanowire, it must be coupled to a superconductor. The electronic coupling between the nanowire and the superconductor induces superconductivity in the nanowire, a phenomenon known as the proximity effect. Following this approach, the first signatures of MZMs were observed in these hybrid systems, characterized by a zero-bias peak (ZBP) in the tunneling conductance spectrum [7].

Of late, it has been found that the coupling depends substantially on the confinement induced by external electric fields. We explore how the change in coupling affects the renormalization of material parameters such as the effective g-factor, spin-orbit interaction etc.

To obtain information about Density of States (DOS) in the proximitized nanowire, we measure the differential conductance dI/dV_{bias} as a function of applied bias voltage V_bias. A magnetic field is applied along the nanowire direction (x -axis).

5.1 Our System

In our system, we consider a nanowire oriented along the x-direction, with a hexagonal cross section in the yz-plane. The hybrid superconductor-nanowire system is described by the BdG Hamiltonian:

$$H = [\,\frac{\hbar^2 k^2}{2m^*} - \mu - e\phi\,]\,\tau_z + \alpha_y\,(\,k_z\,\sigma_x - k_x\,\sigma_z\,)\,\tau_z + \alpha_z\,(\,k_x\,\sigma_y - k_y\,\sigma_x\,)\,\tau_z + \frac{1}{2}\,g\mu_B B\sigma_x + \Delta\tau_x$$

The first term contains contributions from the kinetic energy, chemical potential and electrostatic potential. The second and third terms describe the Rashba spin-orbit coupling with the coupling strength α_i depending on the i-component of the electric field. The fourth term is the Zeeman energy contribution and is proportional to the Landé g-factor. The fifth term represents the superconducting pairing Δ.

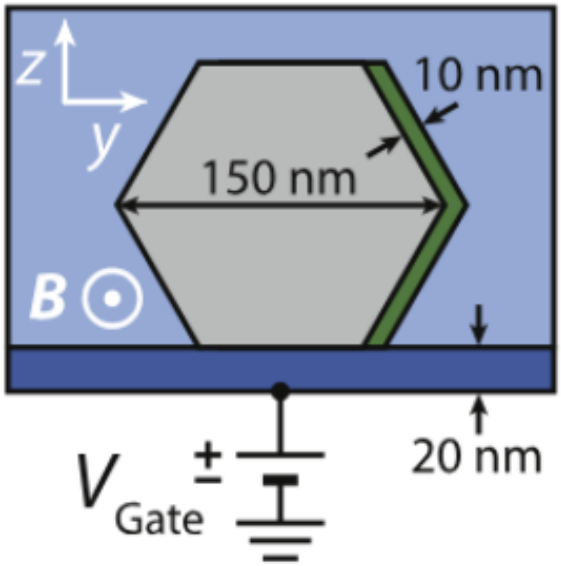

Figure 1: Simplified Geometry that we use in the simulation.

When the coupling between the superconductor and semiconductor is weak (compared to the superconductor's bulk gap), superconductivity can be treated as a constant pairing potential term in the nanowire Hamiltonian, with the induced superconducting gap being proportional to the coupling strength. In cases of strong coupling, the wave functions of the two materials hybridize, requiring a simultaneous solution of the Schrödinger equation in both materials. The orbital effect of the magnetic field can be incorporated via Peierls substitution.

The electrostatic potential in the nanowire cross-section is calculated from the Poisson equation, assuming an infinitely long wire. A fixed potential at the dielectric-substrate interface serves as one boundary condition, while the superconductor provides the second boundary condition, accounting for the work function difference. The mobile charges in the nanowire are approximated using the Thomas-Fermi method, which aligns well with results from self-consistent Schrödinger-Poisson simulations. The calculated potential for a given gate voltage is then incorporated into the Hamiltonian.

5.1.1 Zeeman Term

We define the effective g-factor as $g_{eff} = \frac{2}{\mu_B}|\frac{\Delta E}{\Delta B}|$, so the g_{eff} is essentially proportional to the absolute value of V vs B at the differential conductance

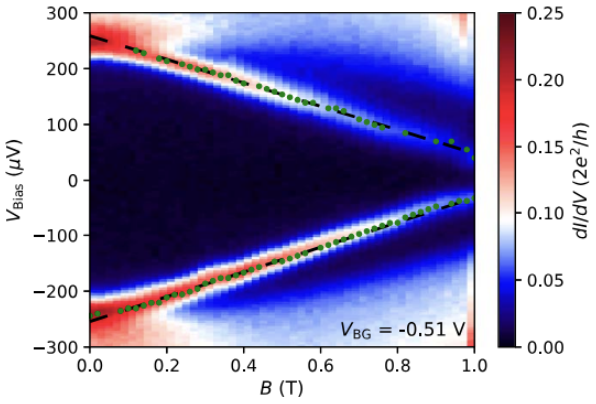

Figure 2: Differential conductance as a function of Vbias and B. Applying a linear fit gives us average slope required

peaks.

5.1.2 Spin-Orbit Coupling

The strength of the coupling is determined by α which is dependent on the material and the electric field [8].

For $\alpha = 0$ there is no coupling between states, and no level repulsion occurs. However as α increases, the levels repel each other, providing us a way to estimate α in the low energy region by the anticrossing energy $2\delta \approx \alpha\pi/l$.

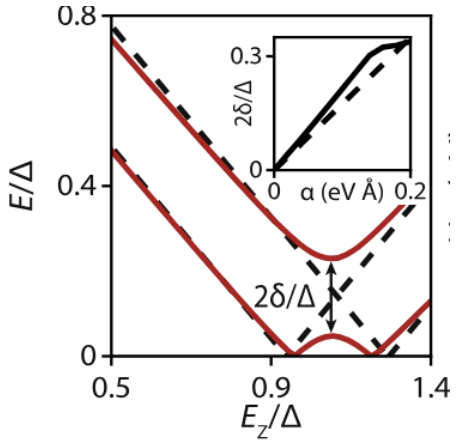

Figure 3: Low Energy Spectrum as a function of Zeeman Energy.

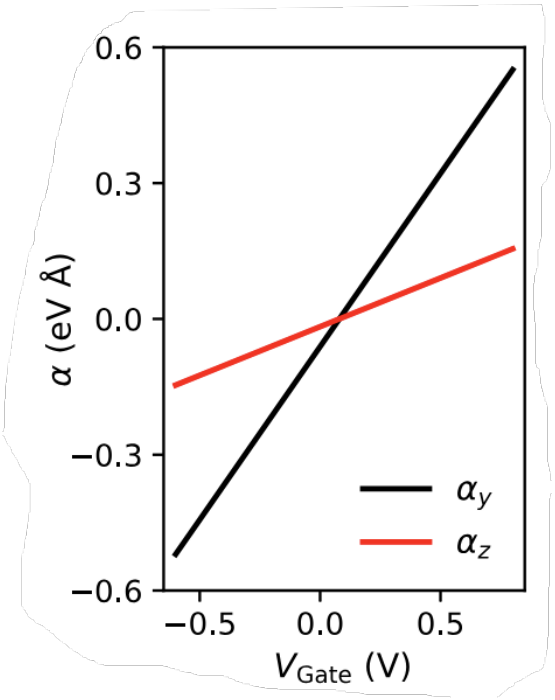

Figure 4: The Rashba coefficients as a function of V$_g ate$

5.2 Results

We make use of the constants provided and the fits obtained out to find the differential conductance as a function of the applied electric field.

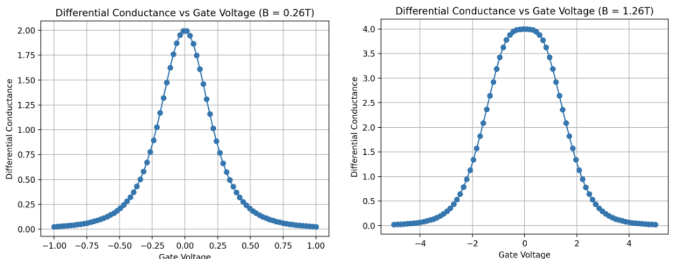

Figure 5: dI/dV as a function of V for different magnetic fields.

In the figures obtained above, we see only one peak and that is a zero bias peak. We can also see the increase in differential conductance magnitude with increase in magnetic field.

On taking into account that the physical parameters are also applied potential and magnetic field dependent, we get similar plots but with a lot more peaks as shown.

Although the trends are clearly visible, the values obtained here do not exactly match those of the paper. This can be attributed to the fact that not all the variables' values were given so I picked up a few from existing literature. Also for the terms that were potential dependent, the exact value of the fit was not explicitly mentioned so I made my best guess.

5.2.1 Conclusions

We saw that appropriate tuning of the repulsion leads to a zero bias peak, mimicking the behaviour expected from Majorana Zero Modes, since MZMs are predicted to lead to a zero energy state, so electrons tunneling into an MZM system should show a ZBP. However this in itself is not enough to sufficiently confirm the existence of a Majorana mode. We need to make further experimental checks, such as the stability of the ZBP in an extended region of parameter space, spanned by relevant gate voltages and magnetic fields.

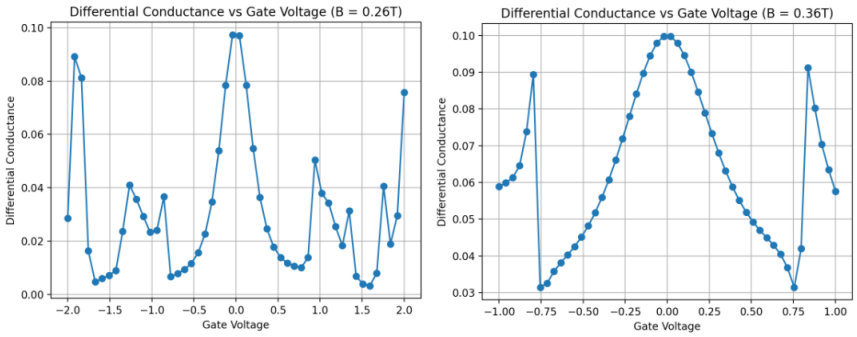

Figure 6: dI/dV as a function of V for different magnetic fields, taking variable parameters into account.

6 References

K. v. Klitzing, G. Dorda, and M. Pepper, Phys. Rev. Lett. 45, 494 (1980).
[2] D. C. Tsui, H. L. Stormer, and A. C. Gossard, Phys. Rev. Lett. 48, 1559 (1982).
[3] J. G. Bednorz and K. A. Müller, Z. Phys. B Con. Matt. 64, 189 (1986).
[4] R. Kozlovsky, "Magnetotransport in 3D Topological Insulator Nanowires", PhD thesis (2020).
[5] M. Zwierzycki, P. A. Khomyakov, A. A. Starikov, K. Xia, M. Talanana, P. X. Xu, V. M. Karpan, I. Marushchenko, I. Turek, G. E. W. Bauer, G. Brocks, and P. J. Kelly, Phys. Status Solidi B 245, 623 (2008).
[6] Lutchyn R M, Sau J D and Das Sarma S 2010 Phys. Rev. Lett. 105 077001
[7] Churchill H O H, Fatemi V, Grove-Rasmussen K, Deng M T, Caroff P, Xu H Q and Marcus C M 2013 Phys. Rev. B 87 241401
[8] Scherübl Z, Fülöp G, Madsen M H, Nygård J and Csonka S 2016 Phys. Rev. B 94 035444